1521-0103/349/3/458–469$25.00
THE JOURNAL OF PHARMACOLOGY AND EXPERIMENTAL THERAPEUTICS

http://dx.doi.org/10.1124/jpet.114.214619
J Pharmacol Exp Ther 349:458–469, June 2014

Preclinical Characterization of Signal Transducer and Activator of Transcription 3 Small Molecule Inhibitors for Primary and Metastatic Brain Cancer Therapy[S]

Hikmat H. Assi, Chris Paran, Nathan VanderVeen, Jonathan Savakus, Robert Doherty, Emanuele Petruzzella, James D. Hoeschele, Henry Appelman, Leda Raptis, Tom Mikkelsen, Pedro R. Lowenstein, and Maria G. Castro

Department of Neurosurgery and Department of Cell and Developmental Biology, University of Michigan School of Medicine, Ann Arbor, Michigan (H.H.A., C.P., N.V., J.S., R.D., P.R.L., M.G.C.); Department of Molecular and Medical Pharmacology, David Geffen School of Medicine, University of California, Los Angeles, Los Angeles, California (H.H.A.); Department of Chemistry, Eastern Michigan University, Ypsilanti, Michigan (E.P., J.D.H.); Department of Pathology, University of Michigan School of Medicine, University Hospital, Ann Arbor, Michigan (H.A.); Department of Biomedical and Molecular Sciences, Queen's University School of Medicine, Kingston, Ontario, Canada (L.R.); and Department of Neurology, Henry Ford Hospital, Detroit, Michigan (T.M.)

Received March 13, 2014; accepted March 31, 2014

ABSTRACT

Signal transducer and activator of transcription 3 (STAT3) has been implicated as a hub for multiple oncogenic pathways. The constitutive activation of STAT3 is present in several cancers, including gliomas (GBMs), and is associated with poor therapeutic responses. Phosphorylation of STAT3 triggers its dimerization and nuclear transport, where it promotes the transcription of genes that stimulate tumor growth. In light of this role, inhibitors of the STAT3 pathway are attractive therapeutic targets for cancer. To this end, we evaluated the STAT3-inhibitory activities of three compounds (CPA-7 [trichloronitritodiammineplatinum(IV)], WP1066 [(*S*,*E*)-3-(6-bromopyridin-2-yl)-2-cyano-*N*-(1-phenylethyl)acrylamide, $C_{17}H_{14}BrN_3O$], and ML116 [4-benzyl-1-{thieno[2,3-d]pyrimidin-4-yl}piperidine, $C_{18}H_{19}N_3S$]) in cultured rodent and human glioma cells, including GBM cancer stem cells. Our results demonstrate a potent induction of growth arrest in GBM cells after drug treatment with a concomitant induction of cell death. Although these compounds were effective at inhibiting STAT3 phosphorylation, they also displayed variable dose-dependent inhibition of STAT1, STAT5, and nuclear factor κ light-chain enhancer of activated B cells. The therapeutic efficacy of these compounds was further evaluated in peripheral and intracranial mouse tumor models. Whereas CPA-7 elicited regression of peripheral tumors, both melanoma and GBM, its efficacy was not evident when the tumors were implanted within the brain. Our data suggest poor permeability of this compound to tumors located within the central nervous system. WP1066 and ML116 exhibited poor in vivo efficacy. In summary, CPA-7 constitutes a powerful anticancer agent in models of peripheral solid cancers. Our data strongly support further development of CPA-7–derived compounds with increased permeability to enhance their efficacy in primary and metastatic brain tumors.

Introduction

Signal transducer and activator of transcription (STAT)3 belongs to the STAT family of proteins whose main function is to relay signals from a specific set of receptor tyrosine kinases and cytoplasmic nonreceptor tyrosine kinases to the nucleus, where gene transcription takes place (Groner et al., 2008). Although the biologic activities of STAT proteins vary, STAT3 has gained notoriety as a signaling hub for multiple oncogenic pathways (Yu et al., 2007; Al Zaid Siddiquee and Turkson, 2008; Brantley and Benveniste, 2008). Constitutive activation of the STAT3 pathway has been noted in several cancer types and typically occurs in response to stimulation by tumor-promoting factors, that is, epidermal growth factor, fibroblast growth factor, interleukin (IL)-6, and Src, among many others (Zhong et al., 1994; Migone et al., 1995; Yu et al., 1995; Bromberg et al., 1998; Abou-Ghazal et al., 2008; Srinivasan et al., 2008). STAT3 activation is mediated through binding to specific transmembrane STAT3/STAT3-dependent receptors. STAT3 becomes activated by Janus kinase (JAK)–dependent tyrosine phosphorylation on a critical tyrosine residue (Tyr^{705}), dimerizing through reciprocal Src homology 2–phosphotyrosine interaction (Prinz et al., 2011). After dimerization, STAT3 translocates to the nucleus and binds to specific sequences within promoter regions, inducing gene transcription. STAT3

This work was supported by National Institutes of Health National Institute of Neurologic Disorders and Stroke [Grants U01-NS052465, U01-NS052465-S1, R01-NS074387, R01-NS057711, MICHR Pilot R14 U040007]; BioInterfaces Institute, University of Michigan [Grant U042841] (to M.G.C.); the National Institutes of Health National Institute of Neurologic Disorders and Stroke [Grants R01-NS054193, R01-NS061107, R01-NS082311, R21-NS084275] and University of Michgan [Grant M-Cube U036756] (to P.R.L.); the National Institutes of Health [Grant UL1-TR000433]; the National Institutes of Health National Cancer Institute [Training Grant T32-CA009676]; the National Institutes of Health National Institute of Neurologic Disorders and Stroke [Grant T32-NS007222]; the National Institutes of Health National Institute of General Medicine Sciences [Grant T32-GM007863]; and the National Institutes of Health through University of Michigan Cancer Center Support [Grant P30-CA046592].
dx.doi.org/10.1124/jpet.114.214619.
[S] This article has supplemental material available at jpet.aspetjournals.org.

contains a second phosphorylation site (Ser^{727}) within its C-terminal region; Ser^{727} phosphorylation is a secondary event after Tyr^{705} phosphorylation, which is required for the maximal transcriptional activity of STAT3. Constitutive activation of STAT3 shown by phosphorylation of the Tyr^{705} residue is present in several types of cancers, including melanomas and gliomas (Niu et al., 2002; Hussain et al., 2007; Kong et al., 2008). Phosphorylation of STAT3 results in the transcription of genes that promote cell proliferation, survival, vascularization, and immunosuppression (Chen et al., 2000; Yu et al., 2007). Inhibition of STAT3 activity in experimental tumor models has provided clear evidence for the role of STAT3 signaling in the growth of tumors, thus becoming an attractive target for cancer therapy (Turkson and Jove, 2000; Stechishin et al., 2013).

Small molecule inhibitors of STAT3 activation have been intensely pursued, that is, sorafenib, a multikinase inhibitor approved for use in advanced renal cell carcinoma and hepatocellular carcinoma patients, has been shown to reduce STAT3 activation (Yang et al., 2008). The preclinical compounds LLL12 (5-hydroxy-9,10-dioxo-9,10-dihydroanthracene-1-sulfonamide) and FLLL32 [(2*E*,2′*E*)-1,1′-(cyclohexane-1,1-diyl)bis (3-(3,4-dimethoxyphenyl)prop-2-en-1-one)], analogs of curcumin, were also effective inhibitors of STAT3 activation (Wei et al., 2011). In addition to downregulating STAT3 activity in human rhabdomyosarcoma cells, these compounds were effective in reducing the growth of MDA-MB-231 breast cancer xenografts in mice (Lin et al., 2010; Wei et al., 2011). However, these are indirect inhibitors of STAT3 as they act by inhibiting the upstream JAK2. Recent clinical trials investigating the use of the JAK1/2 inhibitor AZD1480 (5-chloro-N^2-[(1*S*)-1-(5-fluoro-2-pyrimidinyl)ethyl]-N^4-(5-methyl-1*H*-pyrazol-3-yl)-2,4-pyrimidinediamine) were terminated in phase I when it was reported that the majority of patients experienced adverse events or dose-limiting toxicities (Plimack et al., 2013).

In this study, we evaluated three compounds (CPA-7 [trichloronitritodiammineplatinum(IV)], WP1066 [(*S*,*E*)-3-(6-bromopyridin-2-yl)-2-cyano-*N*-(1-phenylethyl)acrylamide, $C_{17}H_{14}BrN_3O$], and ML116 [4-benzyl-1-{thieno[2,3-d]pyrimidin-4-yl}piperidine, $C_{18}H_{19}N_3S$]; Supplemental Table 1) as inhibitors of STAT3 activation in mouse models of glioma and melanoma. CPA-7 is considered an analog of cisplatin, whose derivatives exhibit variable effects on DNA structure and signal transduction (Boulikas and Vougiouka, 2003). Of these platinum complex derivatives, CPA-7 has been shown to preferentially target STAT3 in transformed cells with potent tumoricidal activity (Littlefield et al., 2008; Zhang et al., 2009). Inhibition of growth in subcutaneous CT26 mouse tumors after CPA-7 administration has also been reported (Turkson et al., 2004). STAT3 inhibition in tumor cells has been shown to upregulate proinflammatory cytokines, activating innate immune responses and dendritic cells, resulting in potent antitumor T-cell responses (Wang et al., 2004). CPA-7 has also been shown to increase IL-1β and tumor necrotic factor-α in N9 microglia, implicating STAT3 inhibition in the modulation of the microglial-mediated immune response (Zhang et al., 2009).

WP1066 is an analog of a previously identified compound [AG490; (*E*)-2-cyano-3-(3,4-dihydrophenyl)-*N*-(phenylmethyl)-2-propenamide] and has been shown to block STAT3 activation by inhibition of the upstream JAK2 signaling (Iwamaru et al., 2007; Kong et al., 2008). We also evaluated ML116, which had recently been identified in a high-throughput screen as a specific and potent inhibitor of STAT3 (Madoux et al., 2010).

Although these compounds have been previously shown to inhibit STAT3 activation in certain transformed cells, their specificity and in vivo efficacy have not been thoroughly evaluated (Hussain et al., 2007; Zhang et al., 2009; Madoux et al., 2010). In this study, we report the tumoricidal activity and specificity of these compounds in a panel of glioblastoma multiforme (GBM) lines, primary GBM cells, and human glioma cells with stem cell properties (Ausman et al., 1970; Sampson et al., 1997; Candolfi et al., 2007; Kumar et al., 2012). In addition, the therapeutic efficacy of CPA-7, WP1066, and ML116 was evaluated in mice bearing intracranial or peripheral GBM (GL26) and melanoma (B16-f0 or B16-f10) tumors. Although the compounds were effective at inducing the death of cancer cells in vitro, ML116 and WP1066 were poor at inhibiting growth of intracranial and peripheral tumors in vivo. Conversely, CPA-7 administration induced tumor regression in mice bearing subcutaneous tumors but was ineffective if the tumors were located within the brain. This differential activity of CPA-7 was attributed to poor blood-brain barrier (BBB) permeability, which was confirmed using immunohistochemistry (IHC), Western blot, and parallel artificial membrane permeability assay (PAMPA).

Materials and Methods

Cell Lines, Antibodies, and Reagents. Cultured cells were obtained from the following vendors: GL26 (American Type Culture Collection, Manassas, VA), HEK-293 (Microbix, Toronto, CA), and B16-f0 (ATCC CRL-6322). HEK-293 cells were cultured in minimal essential medium with supplementation (nonessential amino acids, 1% penicillin-streptomycin, 1% L-glutamine, 10% fetal bovine serum). All other glioma cells were grown in Dulbecco's modified Eagle's medium with supplements. HF2303 (sex unknown) was grown in neurosphere conditions that consisted of Dulbecco's modified Eagle's medium/F12 50:50 medium supplemented with N-2 supplement, 1% penicillin-streptomycin, and a 1% antifungal in addition to having 10 ng/ml recombinant epidermal growth factor and recombinant fibroblast growth factor. Luciferase reporter plasmids were purchased from Promega (Madison, WI). Antibodies for pSTAT3, STAT3, cyclin D,

ABBREVIATIONS: AG490, (*E*)-2-cyano-3-(3,4-dihydrophenyl)-*N*-(phenylmethyl)-2-propenamide; AZD1480, 5-chloro-N^2-[(1*S*)-1-(5-fluoro-2-pyrimidinyl)ethyl]-N^4-(5-methyl-1*H*-pyrazol-3-yl)-2,4-pyrimidinediamine; ANOVA, analysis of variance; BBB, blood-brain barrier; CNS, central nervous system; CPA-7, trichloronitritodiammineplatinum(IV), fac-[$Pt(NH_3)_2Cl_3NO_2$]; DMSO, dimethylsulfoxide; FLLL32, (2*E*,2′*E*)-1,1′-(cyclohexane-1,1-diyl) bis(3-(3,4-dimethoxyphenyl)prop-2-en-1-one); GBM, glioblastoma multiforme; HEK, human embryonic kidney; IFN, interferon; IHC, immunohistochemistry; IL, interleukin; JAK, Janus kinase; LLL12, 5-hydroxy-9,10-dioxo-9,10-dihydroanthracene-1-sulfonamide; LPS, lipopolysaccharide; MG-132, carbobenzoxy-L-leucyl-L-leucyl-L-leucinal; ML116, 4-benzyl-1-{thieno[2,3-d]pyrimidin-4-yl}piperidine, $C_{18}H_{19}N_3S$; NF-κB, nuclear factor κ light-chain enhancer of activated B cells; PAMPA, parallel artificial membrane permeability assay; P_{eff}, effective permeability; PI, propidium iodide; SAR302503, *N-tert*-butyl-3-{5-methyl-2-[4-(2-pyrrolidin-1-yl-ethoxy)-phenylamino]-pyrimidin-4-ylamino}-benzenesulfonamide; STAT, signal transducer and activator of transcription; WP1066, (*S*,*E*)-3-(6-bromopyridin-2-yl)-2-cyano-*N*-(1-phenylethyl) acrylamide, $C_{17}H_{14}BrN_3O$.

and Mcl-1 were purchased from Cell Signaling Technology (Danvers, MA). Anti–Bcl-x_L was purchased from Abcam (Cambridge, UK). Survivin was ordered through Santa Cruz Biotechnologies (Santa Cruz, CA), and anti-actin antibody was purchased from Sigma-Aldrich (St. Louis, MO).

Synthesis, Administration, and Validation of STAT3 Small Molecule Inhibitors. Methods of synthesis, administration, and validation of small molecule inhibitors can be found in Supplemental Table 1; Supplemental Figs. 1 and 2.

Annexin V/Propidium Iodide Flow Cytometry. Glioma cells were seeded onto 12-well plates for apoptosis studies. STAT3 inhibitor was added to the cells after they were fully adhered and incubated for 48 hours before processing. Annexin V/propidium iodide (PI) staining kit was purchased from Invitrogen (Carlsbad, CA). Floating and adherent cells were collected in 5-ml FACS tubes for staining using the manufacturer's suggested protocol. All flow data were collected on a FACS ARIA II cell sorter (BD Biosciences, San Jose, CA) and analyzed with Summit software (Dako North America, Inc., Carpinteria, CA) or Flowjo software (Tree Star Inc., Ashland, OR).

Tumor Models. GL26 glioma cells were originally derived from a female C57BL/6J mouse bearing a chemically induced intracranial neoplasm and used to generate syngeneic mouse glioma models (Ausman et al., 1970). B16-f0 and its more invasive derivative B16-f10 originated as melanoma cell lines used in this study and as alternative models of GBM (Fidler 1973; Raz and Hart, 1980). Intracranial implantation of tumor cells was performed, as previously described (Assi et al., 2013). A brief description of procedures for intracranial and flank tumor models can be found in Supplemental Materials and Methods. All animal experiments conformed to the policies and procedures of the University's Committee on Use and Care of Animals and Unit for Laboratory Animal Medicine at the University of Michigan. Mice used in this study were monitored and humanely euthanized at the first signs of moribund behavior.

Paraffin IHC. A detailed methodology of immunohistochemistry can be found in Supplemental Materials and Methods.

In Vitro Proliferation Assay. Proliferation of glioma cells was determined by measuring ATP levels using the CellTiter-Glo Luminescent Cell Viability Assay provided by Promega. One thousand cells were plated in 100 μl of media and allowed to adhere for 24 hours before the addition of CPA-7, ML116, or WP1066. ATP levels in 96-well plates were measured each day according to manufacturer's instructions (Promega).

Western Blot. Whole-cell lysates were prepared with radioimmunoprecipitation assay buffer supplemented with protease and phosphatase inhibitors, as described previously (Curtin et al., 2009) A more detailed explanation of Western blotting can be found in Supplemental Materials and Methods.

Luciferase Assay for Transcriptional Activity. Transcriptional activity was assessed in stable U251 reporter clones. A detailed description of the process by which reporter cells were generated and used for readout of transcriptional activity can be found in Supplemental Materials and Methods.

PAMPA. PAMPA was performing according to protocols outlined by the manufacturer Pion (Billerica, MA) in accordance with the Vahlteich Medicinal Chemistry Core at the University of Michigan. Permeability assays were performed at pH 7.4. Diffusion of compounds across the lipid layer was measured after a 4-hour incubation period at room temperature.

Statistical Analysis. Error bars represent S.E.M., and asterisks denote statistically significant results. P values of less than 0.05 were considered significant, unless noted otherwise. Statistical significance was calculated using NCSS (Kaysville, UT) or GraphPad software (GraphPad Software, Inc., La Jolla, CA). Dose-response curves and proliferation assays were analyzed by two-way analysis of variance (ANOVA), followed by Tukey-Kramer multiple-comparison test performed using NCSS. Apoptosis experiments and luciferase assays were analyzed using one-way ANOVA, followed by Tukey's test to determine level of significance (GraphPad Software, Inc.). Kaplan-Meier survival curves were analyzed using the Mantel log-rank test used to determine statistical significance in median survival (GraphPad Software, Inc.). A one-tailed Student t test was used to compare p-STAT3 intensity from Western blots of flank and brain tumors treated with CPA-7 (GraphPad Software, Inc.).

Results

Phosphorylated STAT3 Is Differentially Expressed in Cancer Cells. To better understand the extent of STAT3 activation in GBM, we first screened a panel of glioma cell lines of mouse (GL26, SMA560), rat (CNS-1), and human (U251, IN859, HF2303) origin for phosphorylated STAT3 and total STAT3 levels by Western blot (Supplemental Fig. 3). For comparative purposes, whole-cell lysates from HEK-293 cells and two mouse melanoma variants, B16-f0 and B16-f10, were also included. Immunoblotting was performed using an antibody that recognizes the phosphorylated tyrosine 705 residue of STAT3 (pSTAT3). Glioma cells harbored variable levels of STAT3 expression; GL26, U251, and IN859 cells contained the most abundant levels of pSTAT3. Primary human GBM cells cultured in neurosphere conditions were also positive for pSTAT3 expression (HF2303). In contrast, CNS-1, SMA560, and B16-f10 cells had relatively low levels of pSTAT3 similar to HEK-293 cells. The B16-f0 cell line showed the lowest levels of pSTAT3, only detectable after a very long exposure time (B16 Hi exposure; Supplemental Fig. 3).

Inhibition of STAT3 Signaling in Glioma Cells Leads to an Arrest of Cell Growth with Concomitant Induction of Apoptosis. To determine the effects of STAT3 inhibition on cell proliferation in vitro, glioma cells were seeded in 96-well plates and treated the following day with CPA-7, WP1066, or ML116 at drug concentration doses ranging from 100 nM to 100 μM. After 48 hours, intracellular ATP levels were measured and plotted versus drug concentration to obtain dose-response data. All three compounds had a significant effect on inhibiting cell growth in a dose-dependent fashion ($^*P < 0.05$ versus vehicle; Fig. 1A). Barring SMA560 and U251 cells, WP1066 appeared to be the most potent with an IC_{50} of 3–5 μM, depending on the cell type (Fig. 1B). CPA-7 was also very effective at inhibiting the growth of glioma cells, albeit at a slightly higher concentration (IC_{50}: ~3–24 μM). Whereas ML116 did block the proliferation of tumor cells, it was the least effective of the three compounds, requiring higher doses (~1–>50 μM) to elicit comparable effects to that of CPA-7 and WP1066. Using a single dose identified in the dose-response study, we cultured glioma cells in the presence or absence of STAT3 inhibitors and assayed their proliferation over the course of 5–6 days. The amount of intracellular ATP was measured daily and plotted against time; vehicle-treated cells were used as controls. CPA-7 and WP1066 were effective at inhibiting tumor cell growth with high efficacy in vitro ($^*P < 0.05$ versus vehicle; Fig. 1C). Conversely, ML116 was not as effective at inhibiting the proliferation of all cells tested (Fig. 1C). The inhibition of tumor cell growth encountered lends support to the role of STAT3 as a growth-promoting factor in glioma and melanoma cells.

STAT3 is also known to mediate the transcription of genes that regulate apoptosis (Epling-Burnette et al., 2001; Gritsko et al., 2006). To determine whether STAT3 prevents the induction of apoptosis in transformed cells, multiple glioma cell lines were treated with STAT3 inhibitors for 24 hours,

A

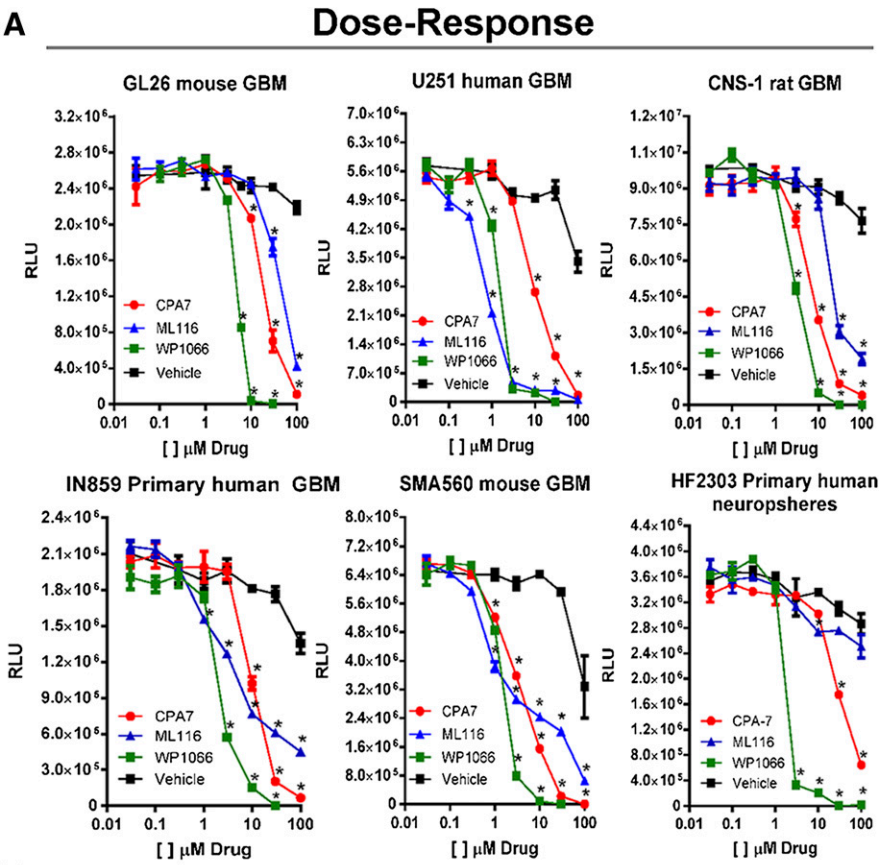

B

IC_{50}	GL26	SMA560	CNS1	IN859	U251	HF2303
CPA-7	17.8μM	2.9μM	6.2μM	9.6μM	8.8μM	23.7μM
WP1066	5.4μM	1.2μM	2.8μM	2.4μM	1.3μM	1.9μM
ML116	33.1μM	2.2μM	22.8μM	6.1μM	0.8μM	N.S.

Fig. 1. Small molecule inhibitors of STAT3 block the proliferation of rodent and human glioma cells in vitro. (A) Dose-response curves were generated by plating mouse (Gl26, SMA560), rat (CNS-1), and human (U251, IN859, HF2303) glioma cells in 96-well plates and adding CPA-7 (red), WP1066 (green), or ML116 (blue) at doses ranging from 10 nM to 100 μM. After 48 hours of treatment, ATP levels were measured in triplicate using the CellTiter Glo kit and plotted versus drug concentration (*$P < 0.05$ versus vehicle; two-way ANOVA followed by Tukey's test). (B) IC_{50} values for CPA-7, WP1066, and ML116 in mouse (Gl26, SMA560), rat (CNS-1), and human (U251, IN859, HF2303) glioma cell lines. (C) Proliferation assays were performed in a similar fashion but were cultured in the presence of a single dose of drug over multiple days. To assess proliferation, ATP levels were measured every day in triplicate over the course of 5–6 days. Growth of glioma cells was dramatically inhibited in response to CPA-7, WP1066, and ML116 in the majority of cell lines tested (*$P < 0.05$ versus vehicle; two-way ANOVA followed by Tukey's test).

after which flow cytometric analysis for annexin V binding and PI retention was performed. This technique permits the visualization of cells in the early (annexin V^+) and later stages of apoptosis or necrosis (PI^+ and annexin V^+). Cells treated with CPA-7 or WP1066 underwent complete apoptosis/necrosis within 24–48 hours, whereas ML116 was less effective at inducing apoptotic cell death in tumor cells, as indicated by flow cytometric analysis (*$P < 0.05$ versus vehicle; Fig. 2).

Western Blot Analysis of STAT3 Phosphorylation and Its Downstream Targets in Tumor Cells Treated with CPA-7, WP1066, and ML116. To better understand the mechanisms by which glioma cells are killed in response to CPA-7, WP1066, or ML116, whole-cell lysates of treated tumor cells were probed by Western blot for pSTAT3, total STAT3, and the following downstream transcriptional targets: Bcl-x_L, survivin, and cyclin D1. The expression of STAT3 and its downstream target genes was evaluated in GL26, SMA560, and CNS-1 rodent glioma cells. CPA-7 or WP1066 was added to the cells at various doses for 24 hours. CPA-7 treatment elicited a dramatic reduction in the levels of p_{Tyr705}STAT3 in all tumor cells tested (Fig. 3A). CPA-7–treated glioma cells were also found to have reduced levels of the antiapoptotic genes *Bcl-x_L* and *survivin*. The expression of the apoptosis inhibitor Bcl-x_L is also STAT3-mediated, with Bcl-x_L blocking apoptosis by preventing the release of cytochrome *c* from mitochondria and subsequently activating caspase (Kharbanda et al., 1997). Survivin can also inhibit apoptosis by binding activated caspase-3 and caspase-7 (Tamm et al., 1998). Cyclin D1, a STAT3 target gene involved in cell cycle progression, was also reduced after CPA-7 treatment, demonstrating a considerable specificity for CPA-7. Whereas WP1066 was also very effective at eliciting the apoptosis of glioma cells, this effect appeared to be less dependent on STAT3. This is best illustrated in GL26 cells in which the addition of WP1066 has no impact on STAT3 phosphorylation or its downstream targets in spite of a strong induction of apoptosis (Fig. 3B). SMA560 cells were also unique in that pSTAT3 levels actually rose with increasing doses of WP1066 before rapidly diminishing at 6 μM, with negligible changes in the expression of Bcl-x_L, surviving, or cyclin D. Unlike GL26 and SMA560 cells, the phosphorylation of STAT3 in rat CNS-1 cells was reduced following WP1066 treatment.

Human U251 GBM cells or primary human GBM neurospheres (HF2303) were also sensitive to STAT3 inhibition, suggesting broad activity of CPA-7 and WP1066 across species (Fig. 3C). ML116 did, in fact, inhibit STAT3 phosphorylation in U251 cells but at much higher concentrations (i.e., 100 μM)

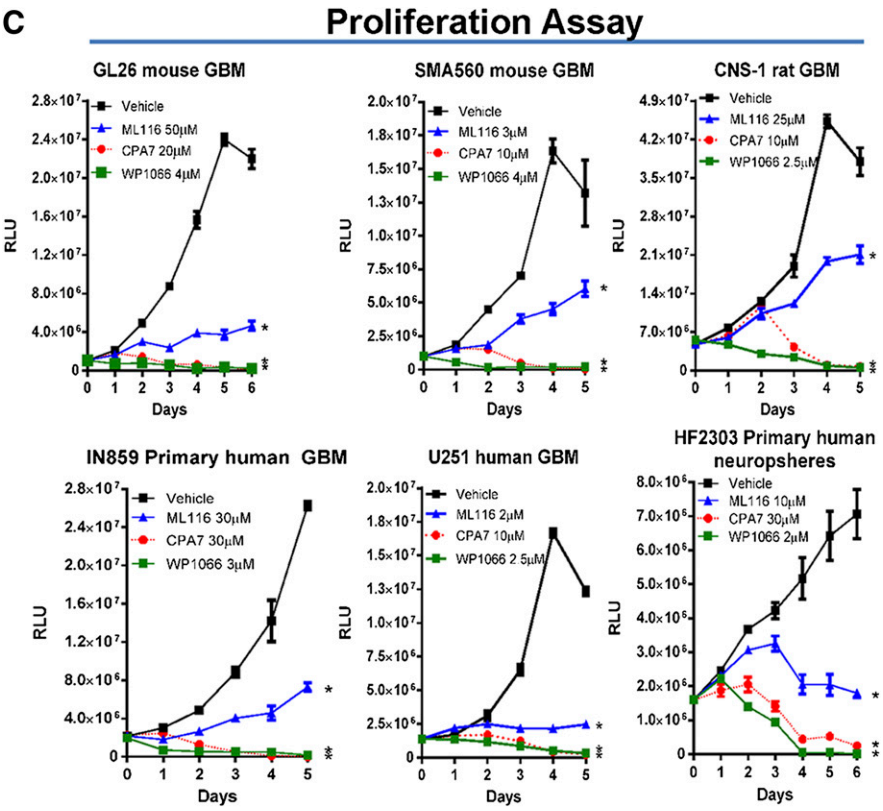

Fig. 1. Continued.

(Supplemental Fig. 4). These results illustrate the changes in STAT3 phosphorylation and downstream proteins elicited by WP1066 and CPA-7. Moreover, our data show that WP1066 can exert antitumor activity independently of STAT3 in rodent GBM cells (Gl26).

Transcriptional Specificity of STAT3 Inhibitors. To determine the specificity of our compounds, transcriptional activity by *STAT3*, *NF-κβ*, *STAT5*, or *STAT1* was assessed in U251 reporter cells, which we genetically engineered to stably express luciferase under the control of promoter regions cis-inducible element, nuclear factor κ light-chain enhancer of activated B cells (NF-κB), STAT5-responsive element, and interferon-stimulated response element, respectively. Transcriptional activity in response to the test compounds was then determined by measuring the bioluminescent signal produced by the cells after drug treatment. Effects on cell viability were factored in to reach a normalized value. CPA-7 and WP1066 were effective at inhibiting the transcriptional activity of STAT3 [$^*P < 0.05$ versus dimethylsulfoxide (DMSO); Fig. 4A]. ML116 also had an effect on STAT3 activity, although this required the use of much higher doses (100 μM). At basal conditions, NF-κB and STAT1 transcriptional activity was low and necessitated the use of exogenous stimuli such as lipopolysaccharide (LPS) or interferon (IFN)-γ ($\dagger P < 0.05$ versus DMSO; Fig. 4B). Pimozide, MG-132 (carbobenzoxy-L-leucyl-L-leucyl-L-leucinal), and nifuroxazide were used as positive control inhibitors of STAT5, NF-κB, and STAT1, respectively. NF-κB–dependent activity, which can modulate STAT3 signaling by secretion of IL-6, was reduced in response to CPA-7 and WP1066 ($^*P < 0.05$ versus LPS; Fig. 4B). STAT5 activity appeared to be modulated in response to WP1066 at doses of 10 μM ($^*P < 0.05$ versus DMSO; Fig. 4C). At very high doses (i.e., 100 μM), CPA-7 exhibited off-target effects and inhibited the activity of IFN-γ–stimulated STAT1 (Turkson et al., 2004) ($^*P < 0.05$ versus IFN-γ; Fig. 4D). WP1066 also inhibited STAT1 activity, albeit at relatively low doses (3 μM and 10 μM).

Therapeutic Efficacy of CPA-7, WP1066, and ML116 in Intracranial and Peripheral Mouse Tumor Models. To generate intracranial tumors, GL26 cells were injected stereotactically into the striatum of syngeneic C57BL/6J. Animals harboring brain tumors were treated with CPA-7, as depicted in Fig. 5, A–D, and humanely euthanized at the first sign of morbidity. Intravenous delivery of CPA-7 into mice bearing intracranial GL26 tumors failed to extend the median survival as mice became moribund at the same time as vehicle-treated animals (Fig. 5B). In mature vertebrates, the BBB can impede the penetration of certain drugs into the central nervous system; therefore, in addition to the intracranial model, we also tested CPA-7 in a peripheral subcutaneous GL26 tumor model. An identical treatment regimen was performed in mice harboring peripheral GL26 tumors (Fig. 5, E–H). In contrast to the intracranial model, mice bearing GL26 flank tumors treated with CPA-7 underwent complete tumor regression ($^*P < 0.05$; Fig. 5F). To fully understand and characterize the safety features of this compound and before clinical implementation, full toxicology assessment is warranted. The tumoricidal efficacy of WP1066 and ML116 was also evaluated in the syngeneic GL26 model, but we did not observe any statistically significant difference in the growth of brain or flank tumors (Supplemental Fig. 5).

CPA-7 shares structural motifs with cisplatin, which is known to have restricted brain permeability. Given its highly

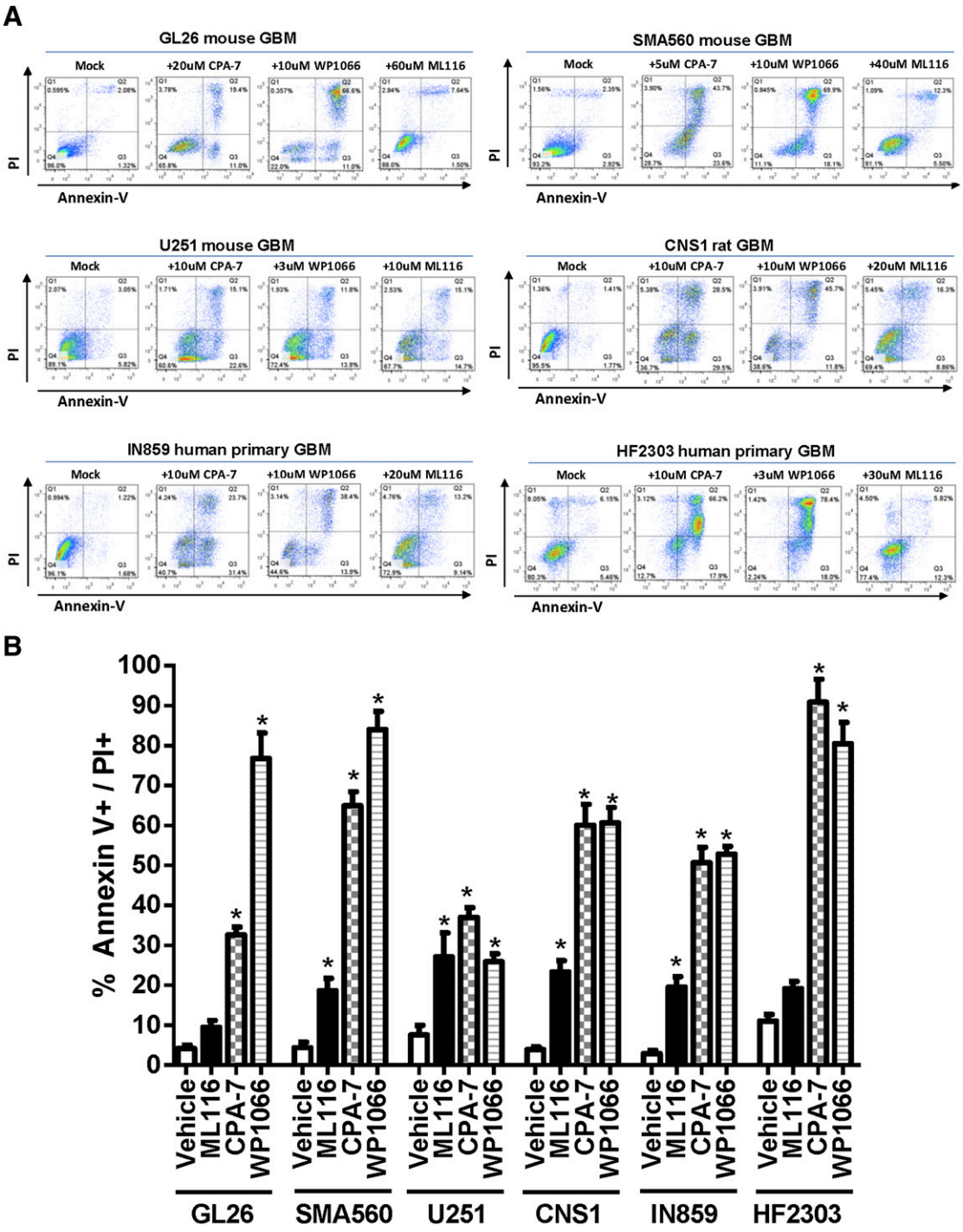

Fig. 2. Inhibition of STAT3 in glioma cells elicits cell death. Glioma cells were cultured with STAT3 inhibitor at the dose indicated for a period of 48 hours in triplicate wells. Cells were analyzed by flow cytometry following staining with annexin V and PI. (A) Representative dot plots from flow cytometric analysis of mouse (Gl26, SMA560), rat (CNS-1), and human (U251, IN859, HF2303) glioma cell lines treated with annexin V and PI presented on the *x*- and *y*-axis, respectively. (B) Cells deemed to be apoptotic (annexin V^+ or annexin V^+/PI^+) were quantified and presented in bar graphs. Inhibition by STAT3 small molecule inhibitors elicits significant levels of cell death ($^*P < 0.05$ versus vehicle; one-way ANOVA followed by Tukey-Kramer multiple-comparison test).

polar structure, we hypothesized that diffusion of CPA-7 into brain tissue would also be limited, justifying its poor therapeutic efficacy in intracranial tumor models. To examine this, C57BL/6 mice bearing either brain or flank tumors (GL26) were treated with CPA-7 for 7 days and then terminally perfused and fixed for IHC. To investigate CPA-7 penetrance and efficacy, tumors were either embedded in paraffin, sectioned, and immunolabeled for pSTAT3 (Fig. 5, C and G) or were harvested for Western blot analysis of whole-tumor lysate (Fig. 5, D and H). GL26 brain tumor-bearing mice treated with CPA-7 had no appreciable difference in levels of STAT3 phosphorylation (Fig. 5C). In contrast, flank tumor-bearing mice treated with STAT3 had reduced levels of pSTAT3 compared with vehicle-treated controls, especially at

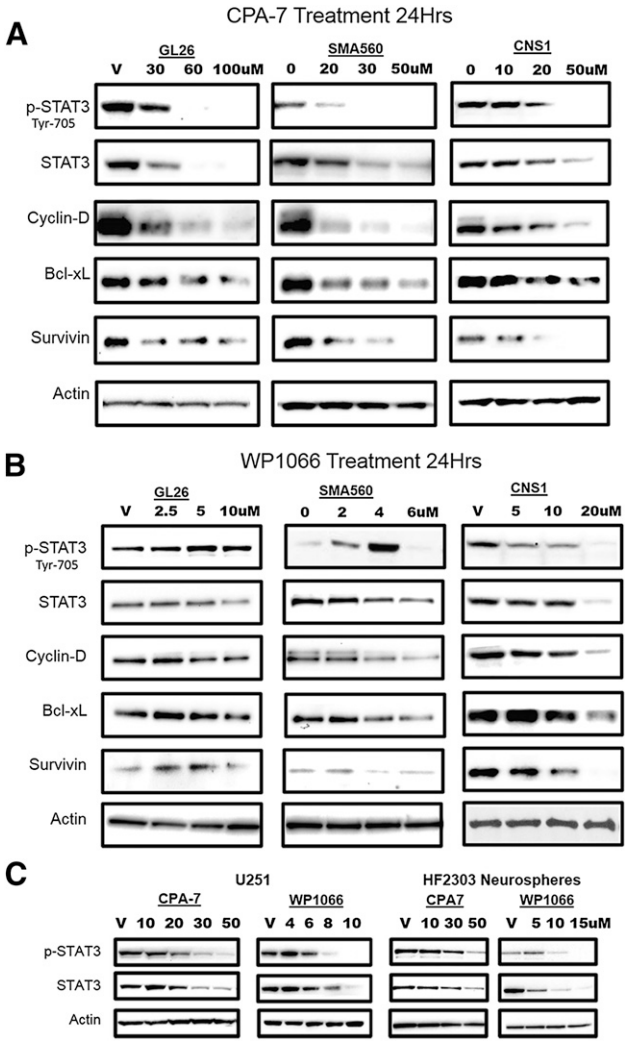

Fig. 3. Decreased expression of STAT3 transcriptional targets is evident in response to small molecule inhibitors. (A–C) Mouse (Gl26, SMA560), rat (CNS-1), and human (U251, IN859, HF2303) glioma cell lines were treated with CPA-7 or WP1066 at the indicated doses for a period of 24 hours, followed by lysis and electrophoretic separation of total proteins on a polyacrylamide gel. Proteins were transferred on a polyvinylidene difluoride membrane and immunoblotted for pSTAT3, total STAT3, or their downstream targets. Levels of actin were used as a loading control.

the tumor borders (Fig. 5G). To further corroborate the IHC data, relative levels of pSTAT3 and total STAT3 were analyzed from whole-tumor lysates by Western blot. Immunoblot analysis of brain tumors treated with CPA-7 corroborated our findings from the IHC, showing no appreciable difference in the expression or phosphorylation of STAT3 in brain tumor lysates (Fig. 5D), whereas flank tumors treated with CPA-7 showed a decrease of pSTAT3 and an associated decrease of total STAT3, as previously demonstrated in vitro ($^*P < 0.05$; one-tailed Student t test; Fig. 5H).

PAMPA is a method used to assess the passive permeability of compounds across an artificial lipid membrane and has been found to correlate with BBB permeability (Avdeef, 2005). As standards for comparison with the STAT3 inhibitors, the effective permeability (P_{eff}) of three control compounds, characterized by their high (verapamil: $P_{eff} = 59.5 \times 10^{-6}$ cm/s), medium (cortisone: $P_{eff} = 23 \times 10^{-6}$ cm/s), and low (theophylline: $P_{eff} = 2 \times 10^{-6}$ cm/s) permeability, was derived simultaneously. WP1066 exhibited high permeability in PAMPA with a P_{eff} value of 54.6×10^{-6} cm/s. Conversely, the permeability of CPA-7 and ML116 was low, with P_{eff} values of 5.1×10^{-6} and 3.7×10^{-6} cm/s, respectively (Supplemental Fig. 6). The poor permeability of CPA-7 observed in PAMPA lends further support to the notion that this particular compound is ineffective for brain tumor models, as it cannot penetrate the blood-brain barrier. ML116 shows a similar pattern of poor permeability as CPA-7, whereas WP1066 shows a high level of permeability in the PAMPA system.

Therapeutic Efficacy and Toxicity of CPA-7, WP1066, and ML116 in Melanoma Models. The therapeutic efficacy of CPA-7, WP1066, and ML116 was also evaluated in the B16-f0 melanoma cell line and its B16-f10 derivative, a more invasive and metastatic clone. These cells form rapidly growing tumors 4–5 days after subcutaneous injection and are prone to ulceration at approximately day 20. The cells can also be used to generate intracranial melanomas. As we observed in the GL26 model, administration of CPA-7 led to an inhibition of tumor growth in both the B16-f10 and the B16-f0 flank tumors ($^*P < 0.05$ versus vehicle; Fig. 6A) but had no therapeutic activity in mice bearing intracranial melanomas (Supplemental Fig. 7). The lack of complete tumor regression in the B16 flank tumor models was attributed to the short therapeutic window as regressing tumor masses became ulcerated and animals had to be euthanized. No notable toxicity was featured in the liver (Fig. 6B) or the spleens (Fig. 6C) in any of the CPA-7–treated animals. We did observe moderate inflammation in the kidneys of CPA-7–treated mice, indicating tissue regeneration in response to a previous injury (Supplemental Fig. 8). A hematologic and serum biochemical analysis (Supplemental Table 2) revealed a depression in several parameters from this cohort, including red blood cells, reticulocytes, white blood cells, lymphocytes, and monocytes (Fig. 6D).

Administration of WP1066 had a small therapeutic effect in the B16-f0 flank tumor model that did not occur in B16-f10 flank tumor-bearing mice (Fig. 6A). In addition, splenic toxicity, characterized by an obliteration of the sinusoids by infiltration of transformed lymphocytes (Fig. 6C), was also evident with WP1066 treatment. Finally, ML116 was the least efficacious of all three compounds, having no discernible therapeutic activity in either intracranial or flank melanoma models (Supplemental Figs. 7 and 9, respectively).

Discussion

Constitutively activated STAT3 has been detected in the majority of advanced stage cancers, including GBM, and is generally correlated with poor prognosis (Abou-Ghazal et al., 2008; Morikawa et al., 2011). STAT3 signaling serves to promote the survival and proliferation of transformed cells by transcriptional regulation of antiapoptotic and cell cycle genes (Brantley and Benveniste, 2008). In this study, we evaluated the in vitro specificity and tumoricidal activity of three STAT3 signaling inhibitors. In addition, the in vivo therapeutic activity and toxicity of these compounds were assessed in both intracranial and peripheral GL26, B16-f0, and B16-f10 mouse tumor models. Our results demonstrate an inhibition of the proliferation of glioma cells in response to CPA-7, WP1066, and ML116. Effects of growth inhibition were associated with an induction of apoptosis in the majority of treated cells. Western blot analysis revealed the highly specific inhibition of STAT3 by

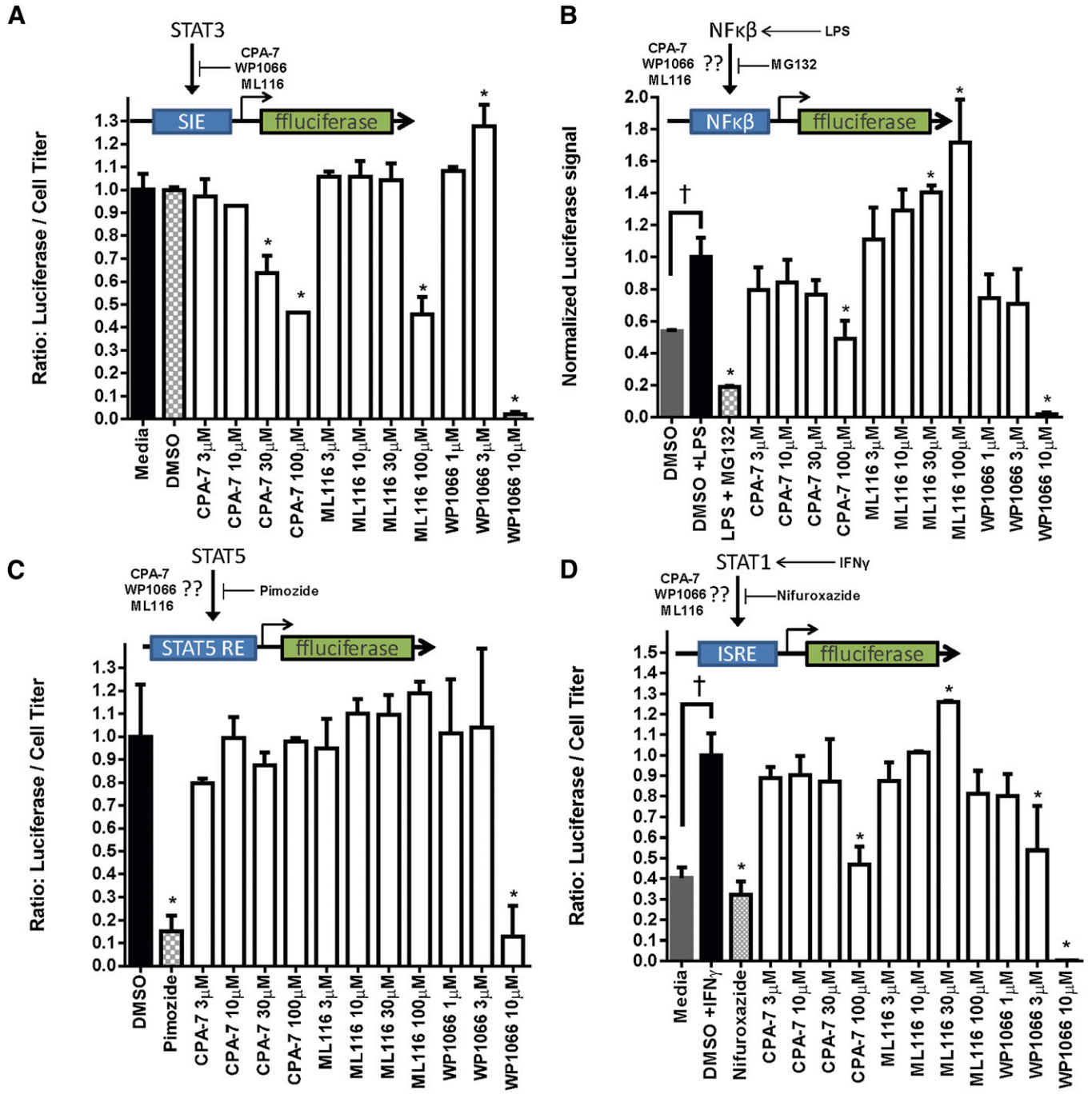

Fig. 4. Transcriptional specificity of STAT3 inhibitors. Transcriptional activity was assessed in triplicate and is represented as the normalized ratio of luciferase signal divided by a separate measurement of ATP levels accounting for cell viability. (A) STAT3-mediated luciferase activity was quantified after a 24-hour treatment with CPA-7, ML116, or WP1066 at the indicated doses (*$P < 0.05$; one-way ANOVA followed by Tukey's test). (B) STAT3 inhibitors or MG132 (known NF-κB inhibitor) were added 1 hour prior to the addition of LPS. LPS was used to stimulate the NF-κB pathway (†$P < 0.05$; one-way ANOVA followed by Tukey's test). NF-κB activity was measured after a 6-hour LPS treatment period (*$P < 0.05$; one-way ANOVA followed by Tukey's test). (C) STAT5-mediated expression of luciferase was quantified after a 6-hour treatment period with pimozide (known STAT5 inhibitor) or STAT3 inhibitors. (D) CPA-7, WP1066, ML116, and nifuroxazide (known pan-STAT inhibitor) were added 1 hour prior to the addition of IFN-γ, which was used to stimulate STAT1 activity. STAT1-specific luciferase expression was measured 6 hours later (*$P < 0.05$; one-way ANOVA followed by Tukey's test).

CPA-7 in various glioma cell lines. This argument was strengthened by the inhibition of downstream targets of STAT3, including Bcl-x_L, survivin, and cyclin D1. In contrast, Western blot analysis of glioma cells treated with WP1066 alluded to a mechanism independent of STAT3 inhibition, as treatment with escalating doses of the compound showed no consistent decrease in pSTAT3 expression or its downstream targets. Using luciferase reporter assays, our results demonstrate inhibition of STAT1 and STAT5 by WP1066. Therefore, WP1066 acts as a JAK2 inhibitor, an observation that has also been noted by other groups (Iwamaru et al., 2007; Kong et al., 2008). We also demonstrate the inhibition of STAT1 in response to high concentrations of CPA-7, which is in agreement with previously published findings (Turkson et al., 2004).

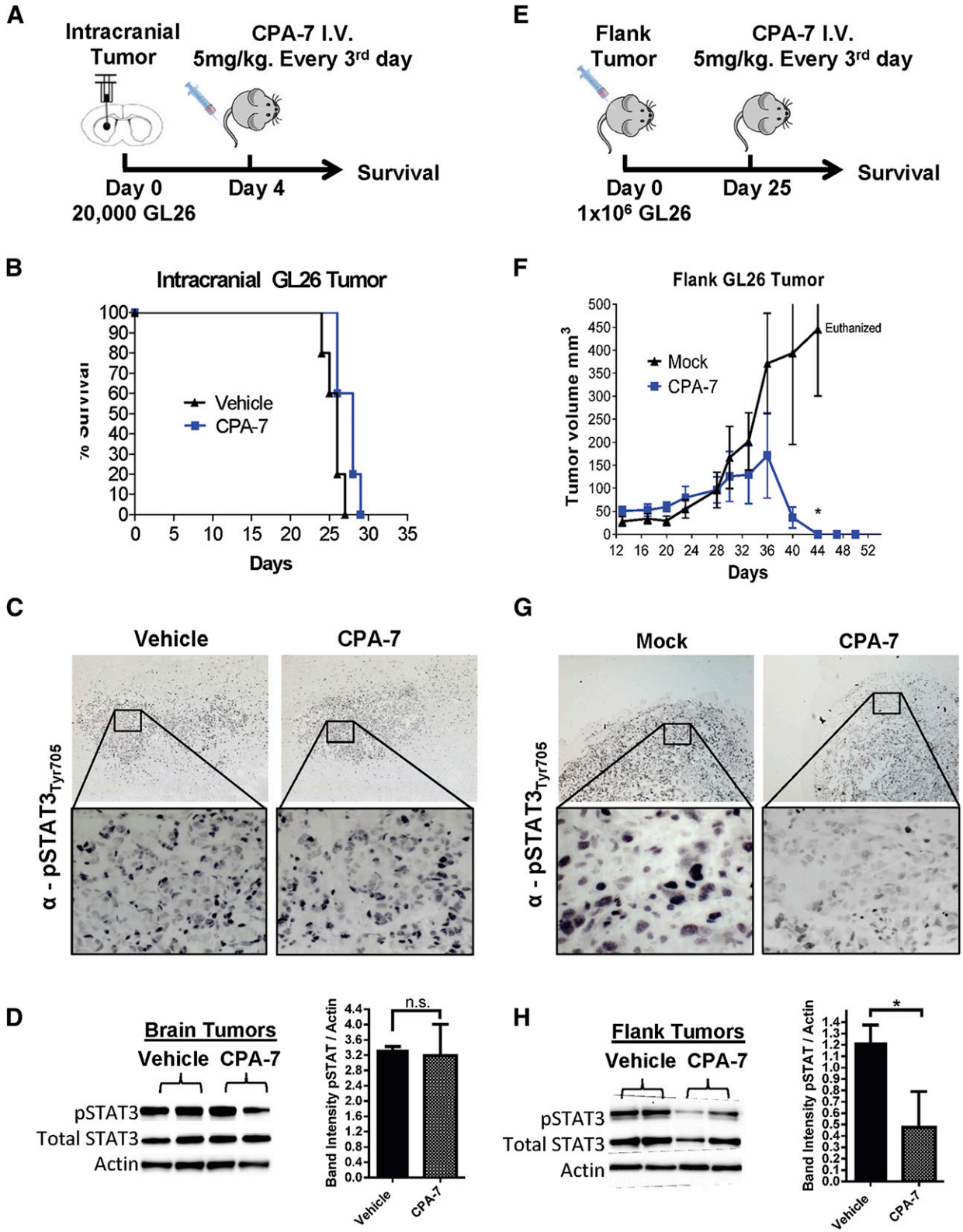

Fig. 5. Therapeutic efficacy of CPA-7 in peripheral subcutaneous tumors and intracranial brain tumors. (A) Twenty thousand GL26 cells were implanted in the striatum of C57BL/6J mice. (B) Mice bearing brain tumors were treated 4 days later with CPA-7 intravenously with no discernible therapeutic effect as seen in the Kaplan-Meier curve (n = 4; 5 mg/kg every 3 days for 15 days). (C) Mice bearing brain tumors were treated with three doses of CPA-7 (5 mg/kg) over a span of 7 days before being harvested for IHC. Paraffin sections were immunostained with an anti-p_{Tyr705}STAT3 antibody and visualized using diaminobenzidine peroxidase. Micrographs were acquired using 5× and 40× objectives. (D) Intracranial tumors from a duplicate treatment cohort were harvested, homogenized, and lysed for Western blot analysis. (E) C57BL/6J mice were injected with 1×10^6 GL26 cells in the hind flank to generate subcutaneous tumors. (F) Mice bearing flank tumors were treated with CPA-7 (n = 5; 5 mg/kg every 3 days for 15 days) when tumors reached an approximate volume of 30–60 mm^3. Plotted values represent the means of tumor volumes ± S.E.M. (*$P < 0.05$; extra sum-of-squares test). (G) Mice bearing GL26 flank tumors were treated three times with CPA-7 (5 mg/kg) over a span of 7 days before being harvested for IHC. Paraffin

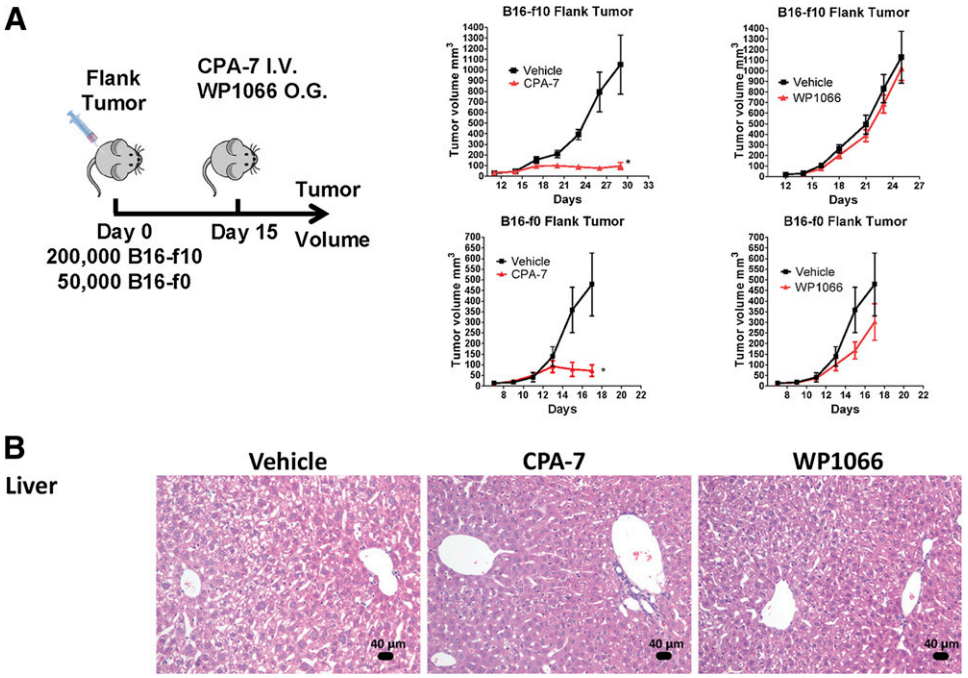

Fig. 6. STAT3 inhibitors are effective at treating peripheral tumors. (A) Fifty thousand B16-f0 or 200,000 B16-f10 melanoma cells were injected in the striatum of C57BL/6J mice. Treatment was initiated with CPA-7 (n = 5; 5 mg/kg i.v. every 3 days) or WP1066 (n = 5; 40 mg/kg oral gavage 5 days on and 2 days off) on day 4 and continued until animals became moribund. Error bars represent ± S.E.M.; *$P < 0.05$; extra sum-of-squares test. (B) B16-f0 flank tumor-bearing mice showed no notable liver toxicity in any animal following treatment with the small molecule STAT3 inhibitors. (C) Whereas no toxicity was observed in the spleens of CPA-7–treated mice, obliteration of the sinusoids by infiltration of transformed lymphocytes was found in 67% of the WP1066-treated animals (n = 3). (D) Hematologic analysis shows a depression in several parameters following treatment with CPA-7, including red blood cells, reticulocytes, white blood cells, lymphocytes, and monocytes when compared with the vehicle. Gray boxes represent normal ranges for this strain.

Whereas WP1066 appeared to exhibit potent cytotoxic activity in vitro, inhibition of STAT3 was only observed in a subset of these cell lines. This phenomenon was best illustrated in GL26 in which addition of WP1066 had no impact on the phosphorylation status of STAT3, despite a robust induction of apoptosis. SMA560 cells were also unique in that pSTAT3 levels actually rose with increasing doses of WP1066 before rapidly declining at a concentration of 6 μM with negligible changes in the expression of cyclin D or Bcl-x_L. In addition, WP1066 elicited significant off-target activity. The off-target effects observed in NF-κB, STAT5, and STAT1 reporter cells suggest that WP1066 is a promiscuous inhibitor. A recent study that used a panel of 368 human kinases (covering ~60% of the human kinome) to profile the specificity of the JAK2 inhibitors ruxolitinib and SAR302503 [*N-tert*-butyl-3-{5-methyl-2-[4-(2-pyrrolidin-1-yl-ethoxy)-phenylamino]-pyrimidin-4-ylamino}-benzenesulfonamide] revealed an inhibition of >30 kinases for ruxolitinib and >50 kinases for SAR302503 (Zhou et al., 2014).

WP1066 has been previously shown to elicit tumor regression in intracerebral B16EGFRvIII and B16-f0 tumor models when used at a dose of 40 mg/kg (Kong et al., 2008). When tested at a dose of 30 mg/kg in an intracerebral B16 melanoma model, this compound did not show therapeutic efficacy (Kong et al., 2008; Hatiboglu et al., 2012). Our results show that this compound was only mildly effective in B16-f10 flank tumors, with negligible effects in GL26 or B16-f0 models, both intracerebral and flank models. The lack of therapeutic efficacy exhibited by WP1066 in our intracranial tumor models cannot be explained by poor BBB permeability; both our PAMPA results and data shown previously indicate that this compound exhibits good diffusion throughout the brain after systemic delivery (Hussain et al., 2007). WP1066 has been approved for a phase I clinical trial in patients with recurrent GBM or metastatic melanoma that will assess the maximum tolerable dose of WP1066 and monitor for any adverse events or dose-limiting toxicities.

CPA-7, in contrast, elicits high therapeutic efficacy in peripheral tumor models (Fig. 5F; Fig. 6A), in addition to high specificity for inhibiting STAT3-mediated signaling (Fig. 3A; Fig. 4). Thus, CPA-7 is a strong candidate for further development as a novel therapeutic strategy for solid cancers. Although CPA-7 does not appear to penetrate the BBB as would be required to treat a tumor located within the central nervous system, alternative therapeutic strategies, such as nanoparticles loaded with CPA-7, could serve as an effective delivery platform. Ultimately, the in vivo inhibition of tumor growth dictates the usefulness of these compounds as anticancer agents. In addition, to avoid toxicity associated with off-target effects, the compounds must be specific to their intended target.

The specificity of CPA-7 for its STAT3 target, as well as its potent antitumor effects in animals harboring peripheral GL26, B16-f0, or B16-f10 tumors that underwent complete tumor regression, highlights its promise as a novel anticancer agent. The lack of therapeutic activity of CPA7 in intracranial tumor models was most likely attributed to the poor diffusion of CPA-7 across the BBB. This was confirmed by IHC and immunoblotting of peripheral and intracranial tumors, in addition to results obtained with PAMPA. To this effect, platinum-based complexes are notorious for having poor brain

sections were immunostained with an anti-p_{Tyr705}STAT3 antibody and visualized using diaminobenzidine peroxidase. Micrographs were acquired using 5× and 40× objectives. (H) Flank tumors from a duplicate treatment cohort were harvested, homogenized, and lysed for Western blot analysis. CPA-7 was effective at reducing the levels of pSTAT3 visualized by IHC or Western blot (*$P < 0.05$; one-tailed Student t test).

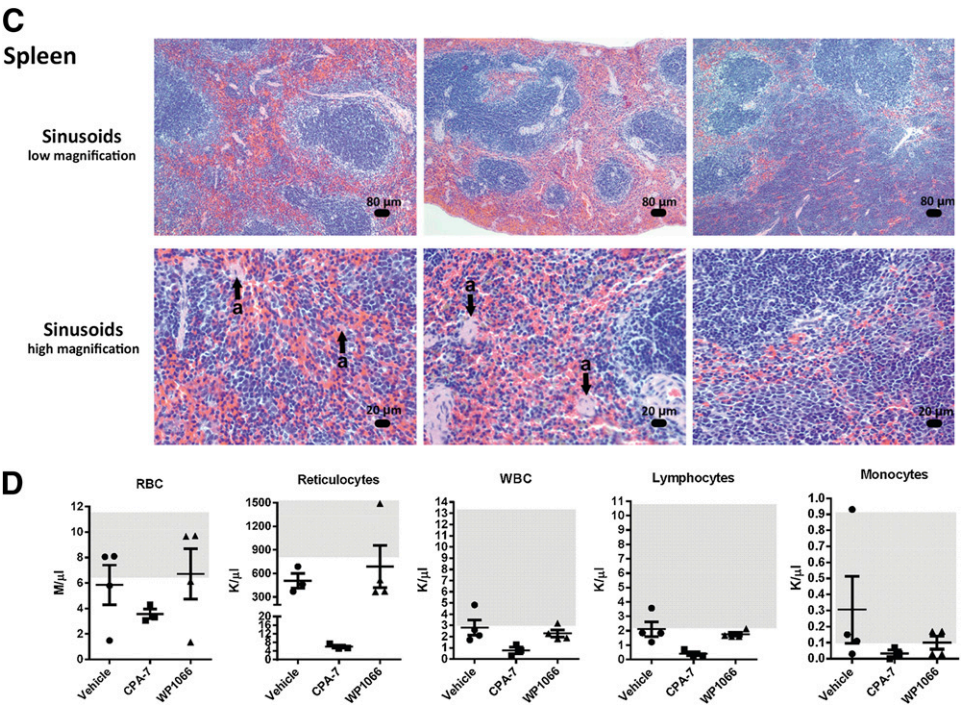

Fig. 6. Continued.

permeability and show poor efficacy for treating central nervous system neoplasms (Gormley et al., 1981; Nakagawa et al., 1994). The success of many clinical trials hinges on the safety of the therapies in question at an efficacious dose. Our results for CPA-7 at the therapeutic dose showed normal liver tissue, normal sinusoids in the spleens of flank tumor-bearing animals treated with the compound, and slight accumulation of protein and a flattening of the epithelial lining of the tubules in the kidneys, indicative of tissue regeneration in response to an injury. To fully understand and characterize the safety features of this compound and before clinical implementation, full toxicology assessment is warranted. In summary, CPA-7 constitutes a powerful anticancer agent in models of peripheral solid cancers. Our data strongly support further development of CPA-7–derived compounds with optimum permeability features to enhance their efficacy in intracranial tumors, that is, GBM.

Furthermore, our data demonstrate several important points, as follows: 1) It highlights the importance of testing chemotherapeutic drugs in vivo, as all compounds exhibited cytotoxicity when tested in rodent tumor cells, human tumor cells, and human tumor stem cells in vitro. 2) It highlights the critical importance of testing drugs in appropriate in vivo models, which reproduce as closely as possible the human condition. Our data conclusively demonstrate that, although CPA-7 shows efficacy when used to treat tumors located in the periphery, when the same tumor is located within the central nervous system, the compound does not exhibit antitumor activity. Furthermore, we demonstrate that this is due to the lack of penetrance of the chemotherapeutic compound into the brain attributed to the presence of the blood-brain barrier (Fig. 5, C, D, G, and H). 3) The data also highlight that thorough and comprehensive testing of novel compounds in the appropriate in vivo animal model is critical before attempting to translate these compounds into the clinical arena (van der Worp et al., 2010; Prinz et al., 2011; Martic-Kehl et al., 2012; Seok et al., 2013; Collins and Tabak, 2014).

Acknowledgments

The authors are grateful for the insight and expertise provided by Drs. Richard Keep and Raoul Kopelman. They are also extremely thankful for the academic leadership and support received from Dr. Karin Murasko and the Department of Neurosurgery; to M. Dahlgren, D. Tomford, and S. Napolitan for superb administrative support; to R. Lemons and M. Dzaman for outstanding technical assistance; and to Phil F. Jenkins for generous support toward the purchase of a Zeiss 3D Scanning Electron Microscope.

Authorship Contributions

Participated in research design: Assi, Paran, VanderVeen, Savakus, Doherty, Lowenstein, Castro.

Conducted experiments: Assi, Paran, VanderVeen, Savakus, Doherty, Petruzzella, Hoeschele, Appelman, Lowenstein, Castro.

Contributed new reagents or analytic tools: Petruzzella, Hoeschele, Raptis, Mikkelsen.

Performed data analysis: Assi, Paran, VanderVeen, Savakus, Doherty, Petruzzella, Hoeschele, Appelman, Lowenstein, Castro.

Wrote or contributed to the writing of the manuscript: Assi, VanderVeen, Doherty, Castro.

References

Abou-Ghazal M, Yang DS, Qiao W, Reina-Ortiz C, Wei J, Kong LY, Fuller GN, Hiraoka N, Priebe W, Sawaya R et al. (2008) The incidence, correlation with tumor-infiltrating inflammation, and prognosis of phosphorylated STAT3 expression in human gliomas. *Clin Cancer Res* 14:8228–8235.

Al Zaid Siddiquee K and Turkson J (2008) STAT3 as a target for inducing apoptosis in solid and hematological tumors. *Cell Res* **18**:254–267.

Assi H, Candolfi M, Lowenstein P, and Castro M (2013) Rodent glioma models: intracranial stereotactic allografts and xenografts, in *Animal Models of Brain Tumors* (Martínez Murillo R and Martinez A eds) vol 77, pp 229-243, Humana Press, New York.

Ausman JI, Shapiro WR, and Rall DP (1970) Studies on the chemotherapy of experimental brain tumors: development of an experimental model. *Cancer Res* **30**: 2394–2400.

Avdeef A (2005) The rise of PAMPA. *Expert Opin Drug Metab Toxicol* **1**:325–342.
Boulikas T and Vougiouka M (2003) Cisplatin and platinum drugs at the molecular level (review). *Oncol Rep* **10**:1663–1682.
Brantley EC and Benveniste EN (2008) Signal transducer and activator of transcription-3: a molecular hub for signaling pathways in gliomas. *Mol Cancer Res* **6**:675–684.
Bromberg JF, Horvath CM, Besser D, Lathem WW, and Darnell JE, Jr (1998) Stat3 activation is required for cellular transformation by v-src. *Mol Cell Biol* **18**: 2553–2558.
Candolfi M, Curtin JF, Nichols WS, Muhammad AG, King GD, Pluhar GE, McNiel EA, Ohlfest JR, Freese AB, and Moore PF, et al. (2007) Intracranial glioblastoma models in preclinical neuro-oncology: neuropathological characterization and tumor progression. *J Neurooncol* **85**:133–148.
Chen T, Wang LH, and Farrar WL (2000) Interleukin 6 activates androgen receptor-mediated gene expression through a signal transducer and activator of transcription 3-dependent pathway in LNCaP prostate cancer cells. *Cancer Res* **60**: 2132–2135.
Collins FS and Tabak LA (2014) Policy: NIH plans to enhance reproducibility. *Nature* **505**:612–613.
Curtin JF, Liu N, Candolfi M, Xiong W, Assi H, Yagiz K, Edwards MR, Michelsen KS, Kroeger KM, and Liu C, et al. (2009) HMGB1 mediates endogenous TLR2 activation and brain tumor regression. *PLoS Med* **6**:e10.
Epling-Burnette PK, Liu JH, Catlett-Falcone R, Turkson J, Oshiro M, Kothapalli R, Li Y, Wang JM, Yang-Yen HF, and Karras J, et al. (2001) Inhibition of STAT3 signaling leads to apoptosis of leukemic large granular lymphocytes and decreased Mcl-1 expression. *J Clin Invest* **107**:351–362.
Fidler IJ (1973) Selection of successive tumour lines for metastasis. *Nat New Biol* **242**:148–149.
Gormley PE, Gangji D, Wood JH, and Poplack DG (1981) Pharmacokinetic study of cerebrospinal fluid penetration of cis-diamminedichloroplatinum (II). *Cancer Chemother Pharmacol* **5**:257–260.
Gritsko T, Williams A, Turkson J, Kaneko S, Bowman T, Huang M, Nam S, Eweis I, Diaz N, Sullivan D et al. (2006) Persistent activation of stat3 signaling induces survivin gene expression and confers resistance to apoptosis in human breast cancer cells. *Clin Cancer Res* 12:11-19.
Groner B, Lucks P, and Borghouts C (2008) The function of Stat3 in tumor cells and their microenvironment. *Semin Cell Dev Biol* **19**:341–350.
Hatiboglu MA, Kong LY, Wei J, Wang Y, McEnery KA, Fuller GN, Qiao W, Davies MA, Priebe W, and Heimberger AB (2012) The tumor microenvironment expression of p-STAT3 influences the efficacy of cyclophosphamide with WP1066 in murine melanoma models. *Int J Cancer* 131:8-17.
Hussain SF, Kong LY, Jordan J, Conrad C, Madden T, Fokt I, Priebe W, and Heimberger AB (2007) A novel small molecule inhibitor of signal transducers and activators of transcription 3 reverses immune tolerance in malignant glioma patients. *Cancer Res* **67**:9630–9636.
Iwamaru A, Szymanski S, Iwado E, Aoki H, Yokoyama T, Fokt I, Hess K, Conrad C, Madden T, and Sawaya R, et al. (2007) A novel inhibitor of the STAT3 pathway induces apoptosis in malignant glioma cells both in vitro and in vivo. *Oncogene* **26**: 2435–2444.
Kharbanda S, Pandey P, Schofield L, Israels S, Roncinske R, Yoshida K, Bharti A, Yuan ZM, Saxena S, and Weichselbaum R, et al. (1997) Role for Bcl-xL as an inhibitor of cytosolic cytochrome C accumulation in DNA damage-induced apoptosis. *Proc Natl Acad Sci USA* **94**:6939–6942.
Kong LY, Abou-Ghazal MK, Wei J, Chakraborty A, Sun W, Qiao W, Fuller GN, Fokt I, Grimm EA, Schmittling RJ et al. (2008) A novel inhibitor of signal transducers and activators of transcription 3 activation is efficacious against established central nervous system melanoma and inhibits regulatory T cells. *Clin Cancer Res* 14: 5759-5768.
Kumar S, Arbab AS, Jain R, Kim J, deCarvalho AC, Shankar A, Mikkelsen T, and Brown SL (2012) Development of a novel animal model to differentiate radiation necrosis from tumor recurrence. *J Neurooncol* **108**:411–420.
Lin L, Hutzen B, Zuo M, Ball S, Deangelis S, Foust E, Pandit B, Ihnat MA, Shenoy SS, and Kulp S, et al. (2010) Novel STAT3 phosphorylation inhibitors exhibit potent growth-suppressive activity in pancreatic and breast cancer cells. *Cancer Res* **70**:2445–2454.
Littlefield SL, Baird MC, Anagnostopoulou A, and Raptis L (2008) Synthesis, characterization and Stat3 inhibitory properties of the prototypical platinum(IV) anticancer drug, [PtCl3(NO2)(NH3)2] (CPA-7). *Inorg Chem* **47**:2798–2804.
Madoux F, Koenig M, Sessions H, Nelson E, Mercer BA, Cameron M, Roush W, Frank D, and Hodder P (2010) *Modulators of STAT Transcription Factors for the Targeted Therapy of Cancer (STAT3 Inhibitors)*, Probe Reports from the NIH Molecular Libraries Program, Bethesda, MD.
Martić-Kehl MI, Schibli R, and Schubiger PA (2012) Can animal data predict human outcome? Problems and pitfalls of translational animal research. *Eur J Nucl Med Mol Imaging* **39**:1492–1496.
Migone TS, Lin JX, Cereseto A, Mulloy JC, O'Shea JJ, Franchini G, and Leonard WJ (1995) Constitutively activated Jak-STAT pathway in T cells transformed with HTLV-I. *Science* **269**:79–81.
Morikawa T, Baba Y, Yamauchi M, Kuchiba A, Nosho K, Shima K, Tanaka N, Huttenhower C, Frank DA, Fuchs CS et al. (2011) STAT3 expression, molecular features, inflammation patterns, and prognosis in a database of 724 colorectal cancers. *Clin Cancer Res* 17:1452-1462.
Nakagawa H, Miyawaki Y, Tokiyoshi K, Tsuruzono K, Yamada M, Kanayama T, and Hayakawa T (1994) [Pharmacokinetics of plasma and cerebrospinal fluid cisplatin in patients with malignant glioma and metastatic brain tumor after selective intraarterial or intravenous and intracarotid administration of etoposide and cisplatin]. *No Shinkei Geka* **22**:35–42.
Niu G, Bowman T, Huang M, Shivers S, Reintgen D, Daud A, Chang A, Kraker A, Jove R, and Yu H (2002) Roles of activated Src and Stat3 signaling in melanoma tumor cell growth. *Oncogene* **21**:7001–7010.
Plimack ER, Lorusso PM, McCoon P, Tang W, Krebs AD, Curt G, and Eckhardt SG (2013) AZD1480: a phase I study of a novel JAK2 inhibitor in solid tumors. *Oncologist* **18**:819–820.
Prinz F, Schlange T, and Asadullah K (2011) Believe it or not: how much can we rely on published data on potential drug targets? *Nat Rev Drug Discov* **10**:712.
Raz A and Hart IR (1980) Murine melanoma: a model for intracranial metastasis. *Br J Cancer* **42**:331–341.
Sampson JH, Ashley DM, Archer GE, Fuchs HE, Dranoff G, Hale LP, and Bigner DD (1997) Characterization of a spontaneous murine astrocytoma and abrogation of its tumorigenicity by cytokine secretion. *Neurosurgery* 41:1365-1372; discussion 1372-1373.
Seok J, Warren HS, Cuenca AG, Mindrinos MN, Baker HV, Xu W, Richards DR, McDonald-Smith GP, Gao H, and Hennessy L, et al.; Inflammation and Host Response to Injury, Large Scale Collaborative Research Program (2013) Genomic responses in mouse models poorly mimic human inflammatory diseases. *Proc Natl Acad Sci USA* **110**:3507–3512.
Srinivasan D, Sims JT, and Plattner R (2008) Aggressive breast cancer cells are dependent on activated Abl kinases for proliferation, anchorage-independent growth and survival. *Oncogene* **27**:1095–1105.
Stechishin OD, Luchman HA, Ruan Y, Blough MD, Nguyen SA, Kelly JJ, Cairncross JG, and Weiss S (2013) On-target JAK2/STAT3 inhibition slows disease progression in orthotopic xenografts of human glioblastoma brain tumor stem cells. *Neuro-oncol* **15**:198–207.
Tamm I, Wang Y, Sausville E, Scudiero DA, Vigna N, Oltersdorf T, and Reed JC (1998) IAP-family protein survivin inhibits caspase activity and apoptosis induced by Fas (CD95), Bax, caspases, and anticancer drugs. *Cancer Res* **58**:5315–5320.
Turkson J and Jove R (2000) STAT proteins: novel molecular targets for cancer drug discovery. *Oncogene* **19**:6613–6626.
Turkson J, Zhang S, Palmer J, Kay H, Stanko J, Mora LB, Sebti S, Yu H, and Jove R (2004) Inhibition of constitutive signal transducer and activator of transcription 3 activation by novel platinum complexes with potent antitumor activity. *Mol Cancer Ther* **3**:1533–1542.
van der Worp HB, Howells DW, Sena ES, Porritt MJ, Rewell S, O'Collins V, and Macleod MR (2010) Can animal models of disease reliably inform human studies? *PLoS Med* **7**:e1000245.
Wang T, Niu G, Kortylewski M, Burdelya L, Shain K, Zhang S, Bhattacharya R, Gabrilovich D, Heller R, and Coppola D, et al. (2004) Regulation of the innate and adaptive immune responses by Stat-3 signaling in tumor cells. *Nat Med* **10**:48–54.
Wei CC, Ball S, Lin L, Liu A, Fuchs JR, Li PK, Li C, and Lin J (2011) Two small molecule compounds, LLL12 and FLLL32, exhibit potent inhibitory activity on STAT3 in human rhabdomyosarcoma cells. *Int J Oncol* **38**:279–285.
Yang F, Van Meter TE, Buettner R, Hedvat M, Liang W, Kowolik CM, Mepani N, Mirosevich J, Nam S, and Chen MY, et al. (2008) Sorafenib inhibits signal transducer and activator of transcription 3 signaling associated with growth arrest and apoptosis of medulloblastomas. *Mol Cancer Ther* **7**:3519–3526.
Yu CL, Meyer DJ, Campbell GS, Larner AC, Carter-Su C, Schwartz J, and Jove R (1995) Enhanced DNA-binding activity of a Stat3-related protein in cells transformed by the Src oncoprotein. *Science* **269**:81–83.
Yu H, Kortylewski M, and Pardoll D (2007) Crosstalk between cancer and immune cells: role of STAT3 in the tumour microenvironment. *Nat Rev Immunol* **7**:41–51.
Zhang L, Alizadeh D, Van Handel M, Kortylewski M, Yu H, and Badie B (2009) Stat3 inhibition activates tumor macrophages and abrogates glioma growth in mice. *Glia* **57**:1458–1467.
Zhong Z, Wen Z, and Darnell JE, Jr (1994) Stat3: a STAT family member activated by tyrosine phosphorylation in response to epidermal growth factor and interleukin-6. *Science* **264**:95–98.
Zhou T, Georgeon S, Moser R, Moore DJ, Caflisch A, and Hantschel O (2014) Specificity and mechanism-of-action of the JAK2 tyrosine kinase inhibitors ruxolitinib and SAR302503 (TG101348). *Leukemia* 28:404-407.

Address correspondence to: Dr. Maria G. Castro, MSRB II, Room 4570, University of Michigan School of Medicine, 1150 West Medical Center Drive, Ann Arbor, MI 48109-5689. E-mail: mariacas@umich.edu